Int. J. Electrochem. Sci., 15 **(2020)** 7545 – 7558, doi: 10.20964/2020.08.71

International Journal of
ELECTROCHEMICAL
SCIENCE
www.electrochemsci.org

Effects of Homoacetogenic Bacteria on the Corrosion Behaviour and Cathodic Protection of AISI 4135 Steel

Xiangju Liu[1,2,3,4], *Yanliang Huang*[1,3,4,*], *Jianzheng Li*[5,6], *Dan Yang*[1,2,4], *Yong Xu*[1,2,4], *Qichao Zhang*[1,2,3,4], *Dongzhu Lu*[1,3,4]

[1] CAS Key Laboratory of Marine Environmental Corrosion and Bio-fouling, Institute of Oceanology, Chinese Academy of Sciences, Qingdao 266071, P. R. China
[2] University of Chinese Academy of Science, Beijing 100049, P. R. China
[3] Open Studio for Marine Corrosion and Protection, Pilot National Laboratory for Marine Science and Technology, Qingdao 266237, P. R. China
[4] Center for Ocean Mega-Science, Chinese Academy of Sciences, 7 Nanhai Road, Qingdao, 266071, P. R. China
[5] School of Municipal and Environment Engineering, Harbin Institute of Technology, Harbin 150090, P. R. China
[6] State Key Laboratory of Urban Water Resource and Environment, Harbin Institute of Technology, Harbin 150090, P. R. China
[*]E-mail: hyl@qdio.ac.cn

Received: 7 December 2019 / *Accepted:* 16 January 2020 / *Published:* 10 July 2020

The corrosion behaviour of high-strength low-alloy AISI 4135 steel was studied in the presence of homoacetogenic bacteria (*Blautia coccoides* GA-1), which catalyse the formation of acetate from H_2 plus CO_2 in their energy metabolism. In addition, the effects of cathodic protection were studied. The chronoamperometry curves showed a negative current density. The minimum current density was approximately −1.5 μA·cm^{-2}. The results revealed that the strain GA-1 could consume 'cathodic hydrogen' and promote the cathodic reaction of AISI 4135 steel, but the hydrogen consumption of strain GA-1 was not the main reason leading to the increase in the corrosion current density.

Keywords: High-strength low-alloy steel, Biocorrosion, Homoacetogenic, Cathodic protection

1. INTRODUCTION

High-strength low-alloy (HSLA) steels are susceptible to hydrogen embrittlement (HE), and HE susceptibility increases with the strength level [1, 2]. In anoxic aqueous surroundings, the hydrogen atoms yielded from water may penetrate into the steel and lead to HE. In marine or soil environments, cathodic protection within a certain range of cathodic potentials is a very effective method to prevent the

corrosion of steels. Under certain conditions (e.g., overprotection and stripping-off the protective coating), the cathodic protection usually applied to constructions immersed in sea water or pipelines buried underground may cause hydrogen charging of the protected metals [3-6].

In addition to cathodic polarization, the presence of microorganisms can also accelerate the corrosion rate and promote hydrogen permeation. Sulfate-reducing bacteria (SRB) have been extensively studied [3, 7-10]. The roles of SRB in iron corrosion can be classified as direct and indirect. In the direct mechanism, according to the depolarization theory, SRB are supposed to stimulate corrosion by the consumption of cathodic hydrogen and the iron-derived electron transfer pathway [11-13]. The indirect corrosion is a chemical attack by hydrogen sulfide or other acidic organisms. The presence of hydrogen sulfide may be responsible for the increase in hydrogen permeation [7, 10]. However, most of the studies concerning microbial processes' effects on hydrogen permeation have focused on hydrogen sulfide while ignoring the direct corrosion. The consumption of cathodic hydrogen by SRB may be one possible way to inhibit hydrogen permeation. Because the metabolites of SRB have been shown to promote hydrogen permeation [7, 10]. The selection of hydrogen consumption bacteria being capable of both consuming hydrogen and inhibit hydrogen permeation is necessary.

Similar to SRB, many microorganisms, such as hydrogen-oxidizing phototrophs, homoacetogens, methanogens, denitrifying bacteria and ferric iron-reducing bacteria, can use hydrogen as an electron donor [14]. In this paper, homoacetogenic bacteria were employed. Homoacetogenic bacteria are strictly anaerobic microorganisms, most of which catalyse the formation of acetate from H_2 plus CO_2 in their energy metabolism (reaction 1) [15]. Furthermore, they can also grow chemoorganotrophically by the fermentation of sugars (reaction 2) [15]. In either case, the sole product of the metabolism is acetate:

$$4H_2 + 2CO_2 \rightarrow CH_3COO^- + H^+ + 4H_2O \quad (1)$$

$$C_6H_{12}O_6 \rightarrow 3CH_3COO^- + 3H^+ \quad (2)$$

The presence of acetic acid may lead to a decrease in the pH value, which may accelerate the corrosion rate. Since the corrosion behaviour of steels affected by homoacetogenic bacteria has rarely been reported, the detailed effects of homoacetogenic bacteria on the corrosion behaviour should therefore be investigated before the hydrogen permeation research. In addition, the effects of the selected bacteria on cathodic protection are also necessary.

2. EXPERIMENTAL

2.1. Specimen, Culture Medium and Bacteria

The HSLA steel AISI 4135 (UNS G41350) used in this study was produced by the Special Steel Department of Beijing Shougang New Steel Co., Ltd., with the chemical composition (wt%) given in Table 1. Short column specimens (Φ10 mm × 10 mm) were used as working electrodes. The back side of the specimens was connected to the copper conductor by tin welding. The specimens were sealed by an epoxy resin except for the front side. The front side of the specimens with an exposure area of 0.785 cm^2 was used as the working surface in electrochemical measurements. Before the experiments, the

working surface of the specimens was abraded with a series of grit papers (400#, 600 #, 800#, 1000#, 1500# and 2000#), cleaned with deionized water (resistivity = 18.2 MΩ·cm) and alcohol in an ultrasonic cleaner and dried by cold-air flow.

Table 1. Chemical composition of AISI 4135 steel (wt%)

C	Si	Mn	P	S	Ni	Cr	Mo	Fe
0.399	0.293	0.509	0.0146	0.0144	0.0804	0.903	0.204	Bal.

The culture medium was composed of culture I and culture II. Culture I contained of 0.5 g NH_4Cl, 0.5 g $MgSO_4 \cdot 7\ H_2O$, 0.189 g $CaCl_2$, 2.25 g NaCl, a 2 mL $FeSO_4 \cdot 7\ H_2O$ solution (0.1% (w/v) in 0.05 mol/L H_2SO_4), a 1 mL trace element solution (containing 10 mL 25% HCl, 1.5 g $FeCl_2 \cdot 4\ H_2O$, 70 mg $ZnCl_2$, 100 mg $MnCl_2 \cdot 4\ H_2O$, 6 mg H_3BO_3, 190 mg $CoCl_2 \cdot 6\ H_2O$, 2 mg $CuCl_2 \cdot 2\ H_2O$, 24 mg $NiCl_2 \cdot 6\ H_2O$, 36 mg $Na_2MoO_4 \cdot 2\ H_2O$ and 990 mL deionized water), a 1 mL selenite-tungstate solution (containing 0.5 g NaOH, 3 mg $Na_2SeO_3 \cdot 5\ H_2O$, 4 mg $Na_2WO_4 \cdot 2\ H_2O$ and 1000 mL deionized water), 2 g yeast extract, 2 g casitone, 0.5 mL Na-resazurin solution [0.1% (w/v)], and 900 mL deionized water. After autoclaving at 121 °C for 20 min, culture II was added, which contained 0.35 g K_2HPO_4, 0.23 g KH_2PO_4, 4 g $NaHCO_3$, 10 mL vitamin solution (containing 2 mg biotin, 2 mg folic acid, 10 mg pyridoxine-HCl, 5 mg thiamine-HCl·2 H_2O, 5 mg riboflavin, 5 mg nicotinic acid, 5 mg D-Ca-pantothenate, 0.1 mg vitamin B12, 5 mg p-aminobenzoic acid, 5 mg lipoic acid and 1000 mL deionized water), 0.3 g L-cysteine-HCl·H_2O and 100 mL deionized water. Culture II was sterilized by filtration.

The homoacetogenic bacteria (*Blautia coccoides* GA-1) was a strictly anaerobic, gram-positive, non-spore-forming bacterium [16, 17]. Before the electrochemical measurements, GA-1 strain was incubated in 100 mL butyl-rubber-stoppered glass bottle with 50 mL culture medium and provided with an anoxic headspace of CO_2/H_2 (20:80, v/v). After being cultured for 12 hours at 37°C, GA-1 strain (2% v/v) was injected into the electrochemical cells via sterile hypodermic syringes.

2.2 Electrochemical Measurements

Glass jars (500 mL) filled with 300 mL of an anoxic sterile culture medium were used as electrochemical cells (Fig. 1). A platinum wire was used as the counter electrode, and a saturated calomel electrode (SCE) served as the reference electrode. The SCE was connected to the medium through a glass salt bridge. The Haber-Luggin capillary tip of the salt bridge was filled with 2% agar and saturated potassium chloride. Apart from the three electrodes, a stainless-steel syringe needle with its tip placed near the surface of the specimen was placed in the same bottle. The needles were used to periodically extract 2 mL of solution for the pH test and were sealed with a plastic plug when not in use. The glass jars and the needles were sterilized in an autoclave at 121°C for 20 min. The three electrodes were sterilized by exposing to ultraviolet for 30 min. Before the electrochemical measurements, the electrochemical cells with sterile medium were placed in a 37°C incubator for approximately 24 hours to verify that the medium was free of bacteria.

The chronoamperometry (CA) data of the working electrodes were detected using an electrochemical workstation (CHI 760C, CH Instruments). The sampling frequency was 1 Hz.

Constant potential pre-polarizations (−0.85 V, −0.95 V and −1.05 V) were applied to the working electrodes using a multi-potentiostat (CHI 1010C, CH Instruments) after GA-1 inoculation. The applied potential was removed before each electrochemical measurement, until the open circuit potential (OCP) stabilized again (The potential change within 60 s was less than ±1 mV). The electrochemical measurements were performed using the electrochemical workstation (Zahner zennium pro, Zahner).

Linear polarization curves were measured by scanning the potential from −20 mV to +20 mV versus OCP at a sweep rate of 1 $mV \cdot s^{-1}$. Electrochemical impedance spectroscopy (EIS) was conducted at a steady-state OCP with an AC perturbation amplitude of 10 mV. The frequency range was from 10 kHz to 10 mHz. Data were collected and fitted using ZSimpwin software. Polarization curves were determined potentiodynamically at a scan rate of 1 $mV \cdot s^{-1}$. The selected scan rate of 1 $mV \cdot s^{-1}$ is assumed to be slow enough for the attached microorganisms to reach their metabolic steady state [13, 18, 19].

All the electrochemical experiments were repeated three times, and the typical results were reported.

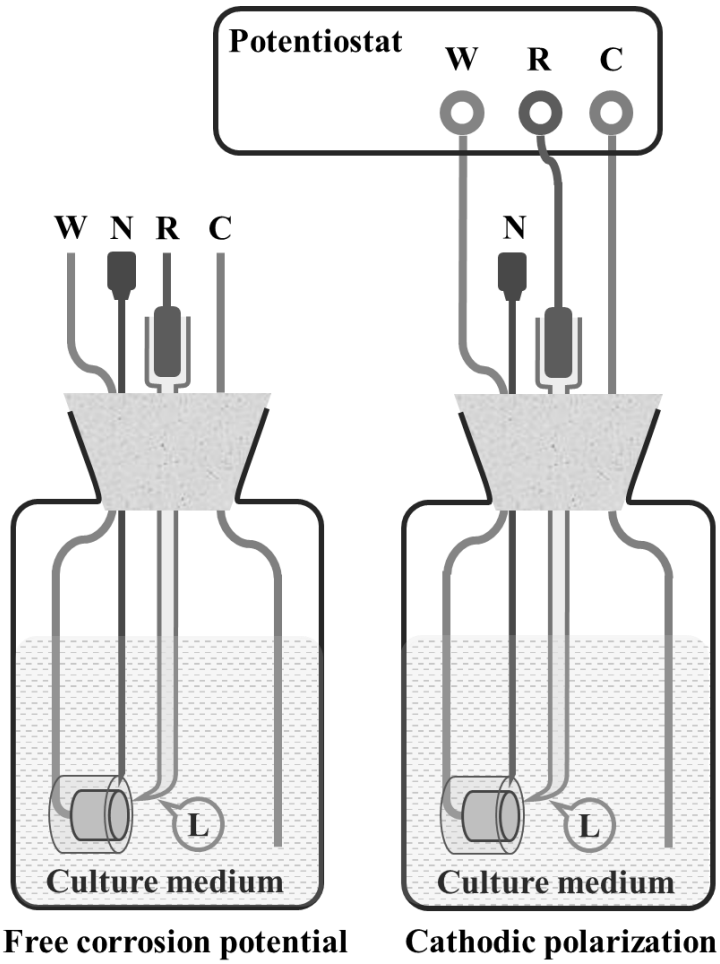

Figure 1. Schematic illustration of the electrochemical cells. W: work electrode, AISI 4135 steel specimen; R: reference electrode, SCE; C: counter electrode, platinum wire; N: stainless steel syringe needle; L: Haber-Luggin capillary tip of the salt bridge.

3. RESULTS AND DISCUSSION

3.1 Growth Curve of Strain GA-1

The process through which the strain GA-1 grew in the culture medium is shown in Fig. 2. Since the strain GA-1 was added at the late exponential stage, the strain GA-1 could quickly enter the exponential growth phase in 2 hours. The number of strain GA-1 cells reached a maximum at approximately 24 hours and then decreased with time. The number of strain cells reduced to half of the maximum at approximately 5 days.

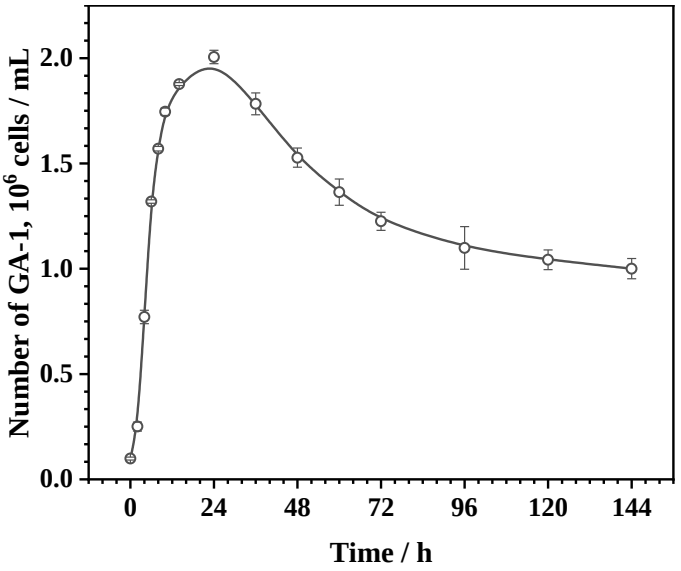

Figure 2. Growth curve of strain GA-1 in the culture medium.

3.2 pH Values

The pH value is an important factor affecting electrode reactions. Since the strain GA-1 could autotrophically reduce CO_2 to acetate with H_2 as an electron donor (reaction 1) by an acetyl-CoA pathway [14, 15, 17], the by-product acetic acid might change the pH value of the culture medium and then affect the electrode reactions. pH measurements were simultaneously carried out during the electrochemical tests. The pH-time curves of the culture medium in the presence of strain GA-1 with the specimen at different potentials are shown in Fig. 3. In general, the pH values remained between 7.3 and 7.6 at different potentials. Since the culture medium did not contain sugar, such as glucose, as an energy source for strain GA-1, the maximum number of strain GA-1 cells was only approximately 2.0×10^6 (Fig. 2). Therefore, the yield of acetic acid was small. In addition, the presence of phosphate buffer pairs in the culture medium could effectively buffer the pH values, causing the low changes in pH value.

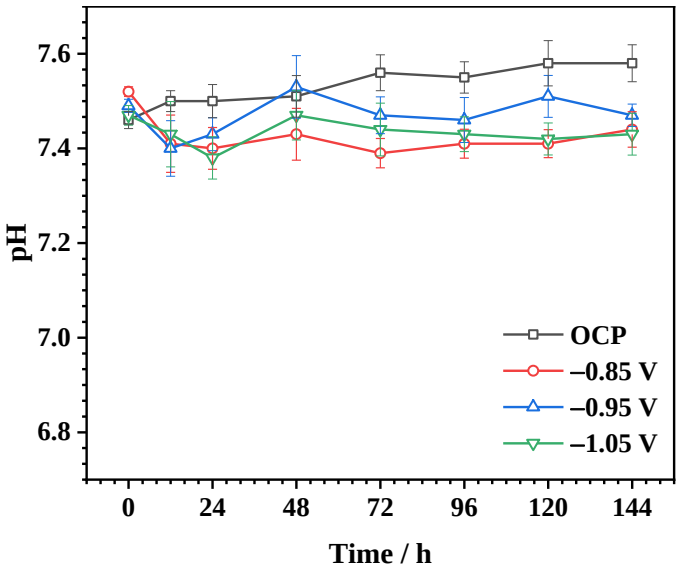

Figure 3. pH-time curves at different potentials.

3.3 Open Circuit Potential

Fig. 4 shows the change in OCP with time in the presence of strain GA-1. The average value of the OCP basically remained unchanged for 12 hours after inoculation with strain GA-1. The average value of the OCP shifted in the positive direction from 12 to 24 hours and then remained steady from 24 to 120 hours. This potential shift in OCP is known as ennoblement [20]. The exact mechanism of ennoblement remains unsolved [20].

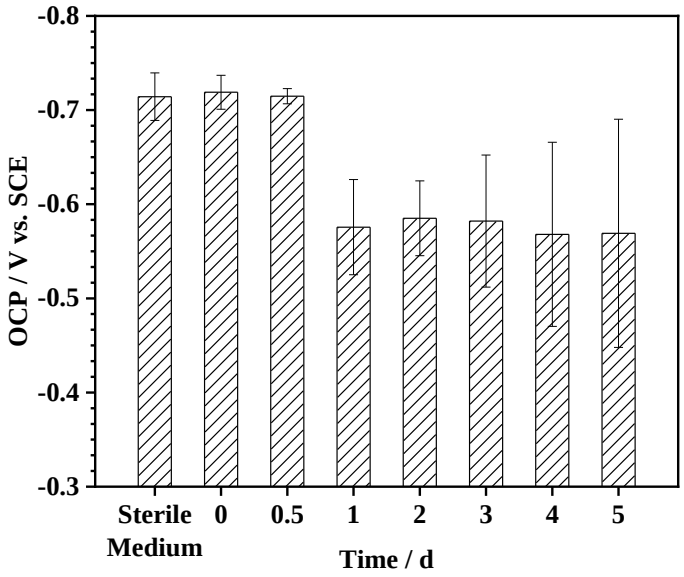

Figure 4. OCP of AISI 4135 steel in sterile and strain GA-1-inoculated culture medium.

Complex deposits of microbial cells, extracellular polymers, and organic and inorganic compounds that accumulate on the metal surface accelerate corrosion by changing the electrochemical

behaviour of the metal [21]. These factors collectively could result in ennoblement [20]. Different studies have attempted to understand whether there is a direct link between biofilm formation and ennoblement [12, 22-24]. J. Wang et al. [22] found that the bacteria attachment and growth of biofilms were the cause for the ennoblement of the OCP of passive metals. L. Yu et al. [12] reported that a sulfate-reduction bacteria (SRB) biofilm rather than their metabolic product was directly related with the ennoblement of the OCP of carbon steels.

3.4 Chronoamperometry Measurements

Chronoamperometry is an effective way to detect the charge transfer process between steel and the biofilm [12]. In this paper, the AISI 4135 steel specimen was potentiostatically controlled at −0.76 V (the free corrosion potential of AISI 4135 steel in sterile medium) to identify the bioelectrical activity of adherent strain GA-1 cells. The current density-time curve is shown in Fig. 5. The current density curve was essentially below the zero line.

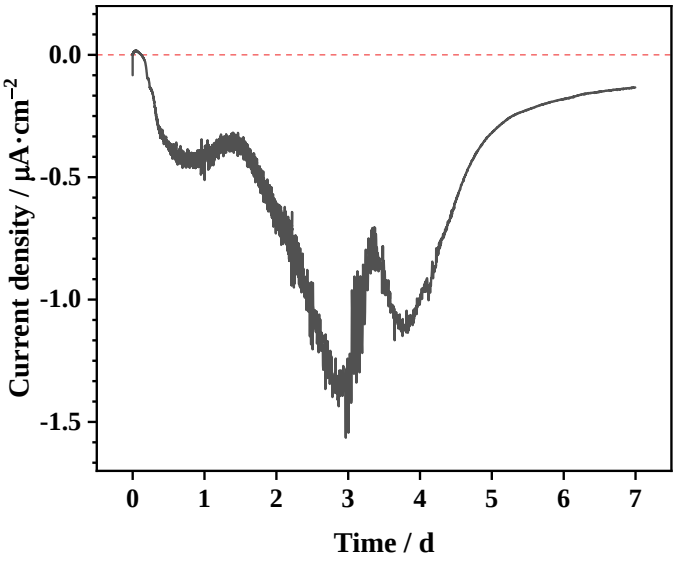

Figure 5. Current output when AISI 4135 steel was potentiostatically controlled at −0.76 V in the culture medium with strain GA-1.

The negative current density means that the electron transfer direction was from the AISI 4135 steel to strain GA-1 cells or to the electroactive material around the electrode. This result proved that the presence of strain GA-1 could directly or indirectly obtain electrons from the AISI 4135 steel specimen, leading to the ennoblement of the OCP (Fig. 4). Strain GA-1 can grow not only autotrophically but also heterotrophically by decomposing organic matter [17]. When the culture medium contained organic matter available for the strain, the strain was more inclined towards heterotrophic growth [17]. Although there was no sugar in the fresh medium as a carbon source, the presence of yeast extract and casitone in the culture medium could also provide available organic matter for the heterotrophic growth of strain GA-1. Therefore, in the early stage of the culture, the strain GA-1 were undergoing mixotrophic growth.

The proportion of hydrogen consumption was small. With the growth of strain GA-1, the organic matter was depleted. The autotrophic growth of strain GA-1 then dominated, leading to the increased hydrogen consumption. The minimum current density reached −1.5 μA·cm^{-2} near the third day. The ability of strain GA-1 to obtain energy from AISI 4135 steel gradually diminished after 4 days. This might have been caused by the decrease in cell number and the depletion of essential elements for growth in the culture medium, compared with the growth curve shown in Fig. 2.

3.5 Linear Polarization Measurements

Fig. 6(a) shows the change in R_{LPR} with time in the presence of strain GA-1 at OCP and after the removal of different pre-polarization potentials**.** At OCP without pre-polarization, with the growth and metabolism of strain GA-1, R_{LPR} decreased in 24 hours and then increased slightly. The applied cathodic pre-polarization significantly increased the values of R_{LPR}.

According to the Stern-Geary equation:

$$i_{corr} = B \cdot R_{LPR}^{-1} \qquad (3)$$

where i_{corr} is the corrosion current density and B is an empirical constant, which is approximately equal in the same system.

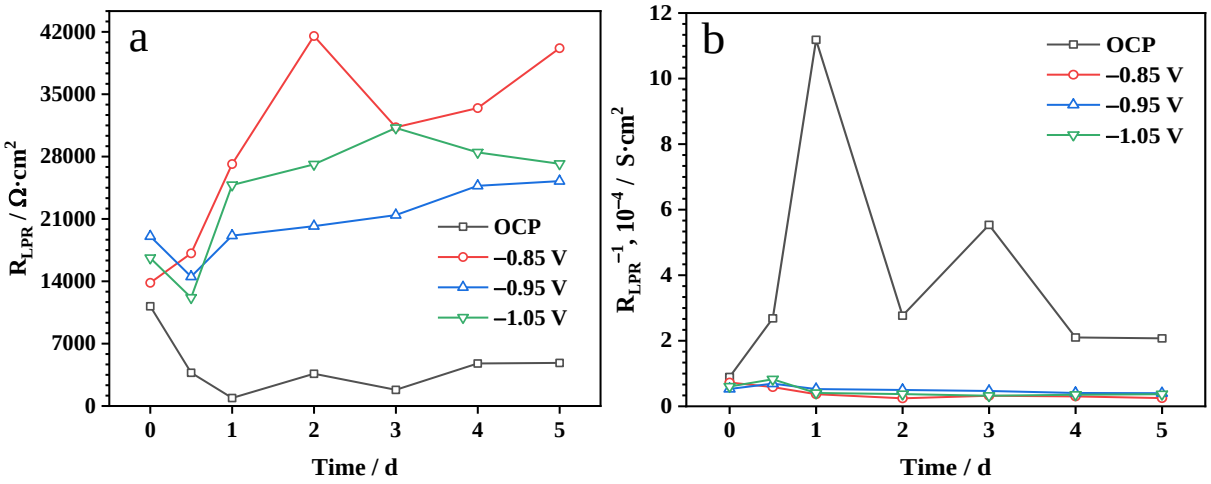

Figure 6. Linear polarization resistance R_{LPR} (a) and R_{LPR}^{-1} (b) curves of AISI 4135 steel in strain GA-1-inoculated medium at OCP without cathodic pre-polarization and after the removal of different pre-polarization potentials.

The corrosion rate could be evaluated by R_{LPR}^{-1} [25]. R_{LPR}^{-1}-time curves are shown in Fig. 6(b). Apparently, the growth and metabolism of strain GA-1 could promote the corrosion process of AISI 4135 steel. In addition, it seems that the protection effects were similar at −0.85 V, −0.95 V and −1.05 V pre-polarization potentials. The corrosion rate of the specimens at OCP without cathodic pre-polarization was always 5 times that under pre-cathodic protection; that is, the protection efficiency was more than 80% for cathodic pre-polarization.

3.6 EIS Measurements at Stable OCP

The EIS measurements were carried out at stable OCP. The Nyquist and Bode plots for AISI 4135 specimens in the presence of strain GA-1 under different conditions and at different exposure times are shown in Fig. 7. The results demonstrated the variation in the impedance values when the samples were exposed for different lengths of time.

Here, the impedance of the steel at low frequencies (e.g., less than 10 mHz) is related to the polarization impedance (R_p). The R_p value reflects the corrosion reaction of the steel and is inversely proportional to corrosion current and hence to corrosion rate [26]. The resistance of the steel at high frequencies (e.g., more than 10 kHz) is related to the electrolyte resistance (R_s) [27]. The *R*s value represents the electrolyte resistance of the solution.

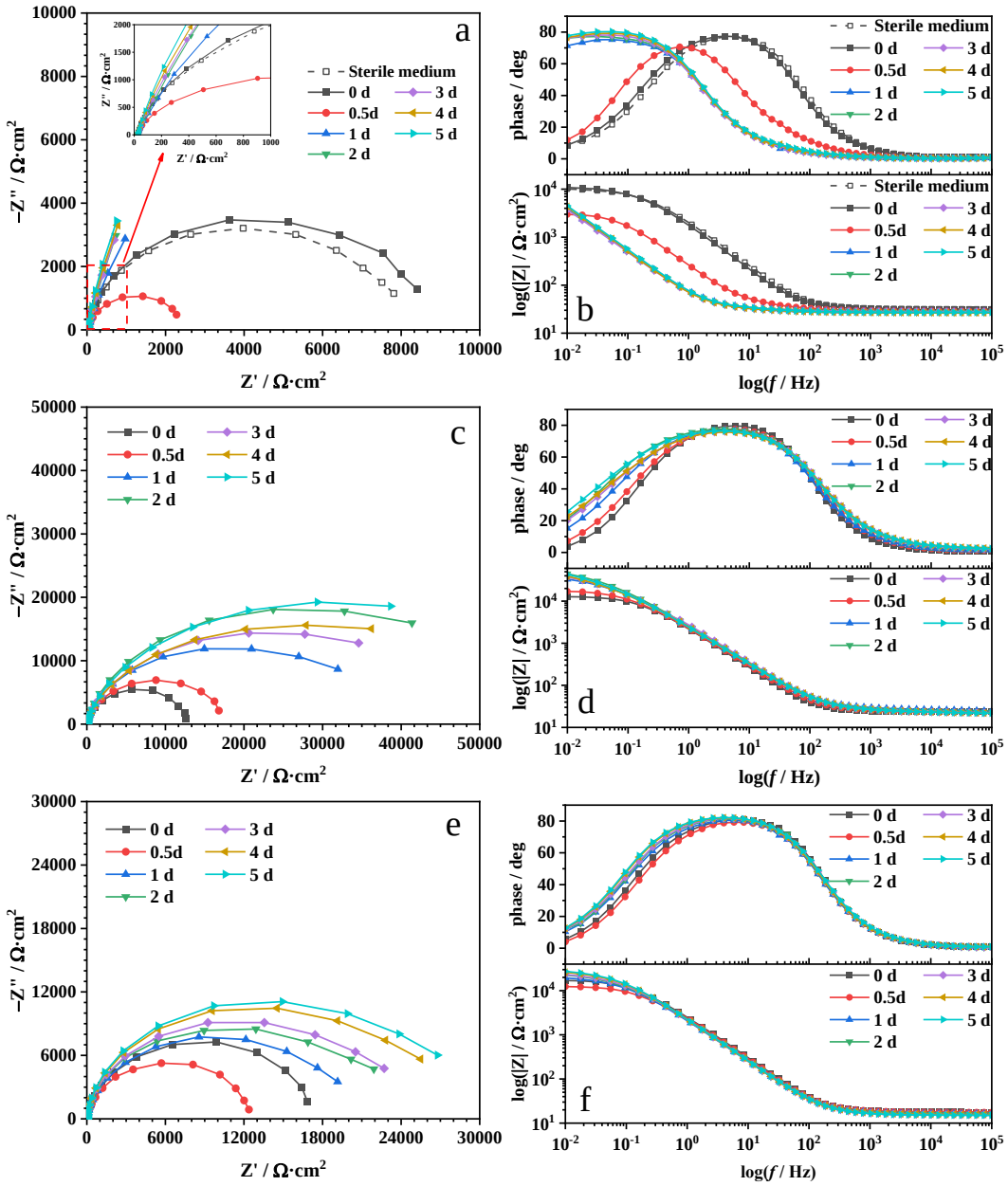

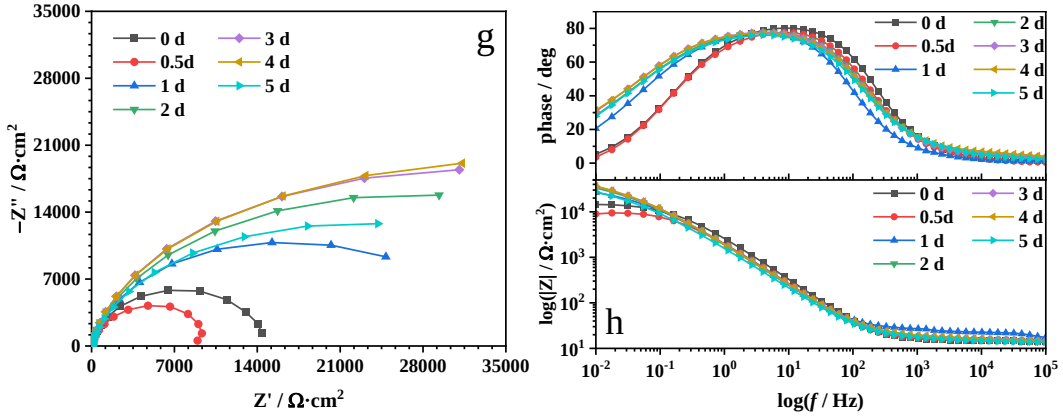

Figure 7. Nyquist and Bode plots for the specimens in the presence of strain GA-1 at OCP without cathodic pre-polarization and after the removal of different pre-polarization potentials with time. OCP (a, b), −0.85 V (c, d), −0.95 V (e, f), and −1.05 V (g, h).

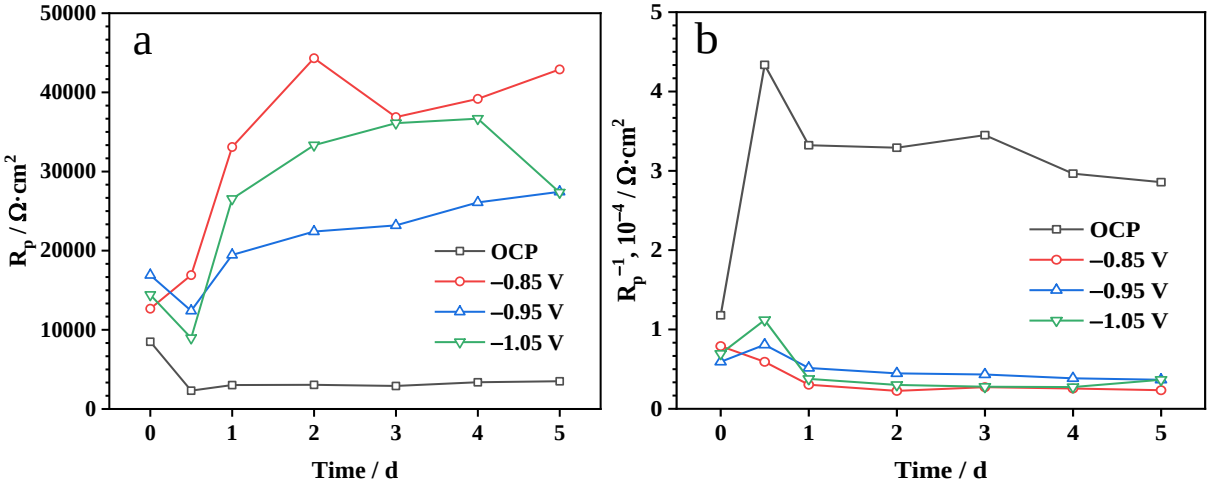

Figure 8. R_p (a) and R_p^{-1} (b) curves of AISI 4135 steel in strain GA-1-inoculated medium at OCP without cathodic pre-polarization and after the removal of different pre-polarization potentials.

In Bode plots, the polarization impedance (R_p, Ω·cm^2) of the steel can be roughly calculated as [27, 28]:

$$R_p = |Z|_{10\ mHz} - |Z|_{10\ kHz} \qquad (4)$$

where $|Z|_{10\ mHz}$ (Ω·cm^2) and $|Z|_{10\ kHz}$ (Ω·cm^2) are the impedance values at 10 mHz and 10 kHz, respectively.

Since the equation for R_p does not contain R_s, its value was more accurate than R_{LPR}. This approach has been widely used in the literature [27-29]. The corrosion current density can be obtained by equation (7), where R_{LPR}^{-1} is replaced by R_p^{-1}. The R_p and R_p^{-1} curves are shown in Fig. 8. The changing trends of R_p and R_p^{-1} were generally consistent with those of R_{LPR} and R_{LPR}^{-1}, respectively.

3.7 Potentiodynamic Polarization Curve Measurements

The cathodic polarization curves of AISI 4135 steel are shown in Fig. 9. The cathodic polarization curves were basically straight in the strongly polarized zone (η>118 mV) [30]. These results revealed that the cathodic reactions of the AISI 4135 steel specimen were controlled by electrochemical polarization. The fitted Tafel slopes of the cathodic curves (b_c) and corrosion current density (i_{corr}) are shown in Fig. 10.

The corrosion current density of AISI 4135 steel increased within 24 hours and gradually decreased from day 1 to day 5 with the growth and metabolism of strain GA-1 without cathodic pre-polarization (shown in Fig. 10(b)). It seems that the corrosion rate had a strong relationship with the number of strain GA-1 cells (Fig. 2). According to Fig. 5, the ability of strain GA-1's to consume hydrogen was weak within 12 hours with the current density being 0.46 μA·cm^{-2}. The i_{corr} value reached 7.76 μA·cm^{-2} at 12 hours after strain GA-1's inoculation, as shown in Fig 10(b). Thus, the hydrogen consumption of strain GA-1 was not the main reason leading to the increase in corrosion current density.

It can be seen in Fig. 3 that the growth of strain GA-1 led to a reduced change in the pH value. However, the local acidification of the steel surface may have been caused by the acetic acid produced by adherent strain GA-1 cells, although the solution contained phosphate buffer pairs. J.W. Sowards et al. [31] reported that extensive pitting corrosion was observed on the 1080 cold-drawn steel (ASTM A108) surface in the presence of acid-producing bacteria, and the corrosion rate was 0.402-0.876 mm/y. A. Heyer et al. [32] found that acidic bacteria generated holes with 0.2-0.9 μm in depth and 4-9 μm in width on a metallic coating. Therefore, producing acidic acid could cause significant corrosion.

The AISI 4135 steel specimens were well protected when the cathodic pre-polarization potentials were applied. The corrosion current density of the specimens after the −0.85 V pre-polarization was 8.6 times smaller than that of the specimens without pre-cathodic protection. The pre-cathodic protection effects were similar at −0.85 V, −0.95 V and −1.05 V polarization potentials.

It is known that a more negative polarization potential may lead to a strong hydrogen evolution reaction. The generated hydrogen might penetrate into steels and lead to the hydrogen embrittlement [33-36]. Therefore, further research needs to be conducted to confirm the desired protection potential with a hydrogen permeation test.

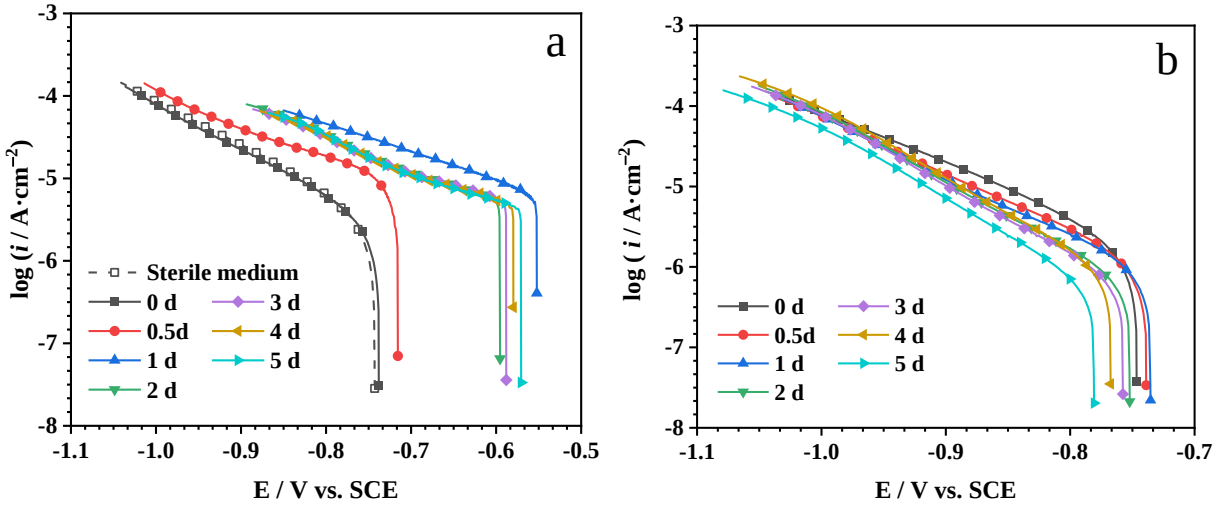

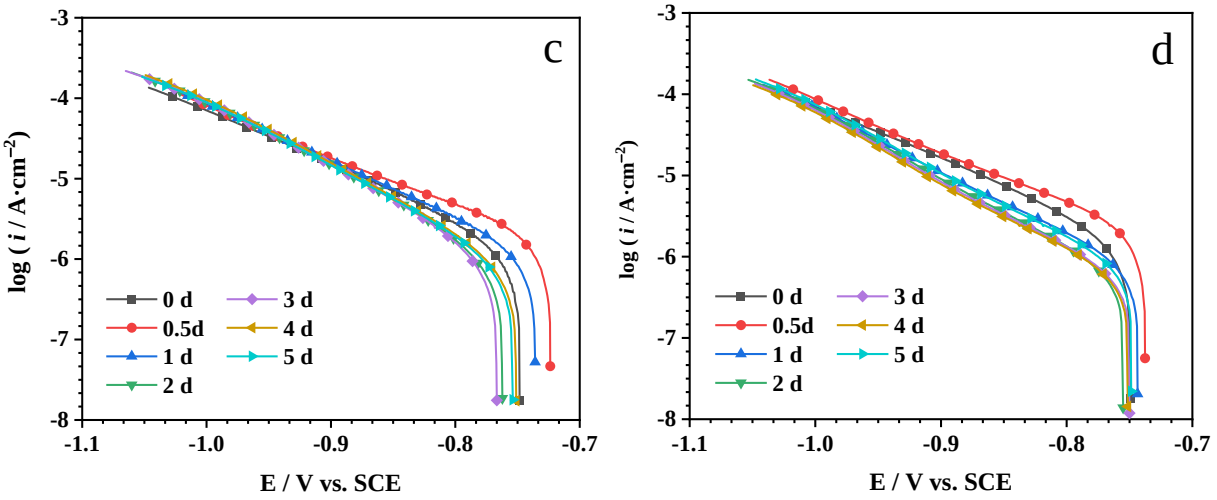

Figure 9. Cathodic polarization curves for the specimens in the presence of strain GA-1 with time at OCP and after different pre-polarization potentials. a: OCP without cathodic pre-polarization, b: pre-polarized at −0.85 V, c: pre-polarized at −0.95 V, and d: pre-polarized at −1.05 V.

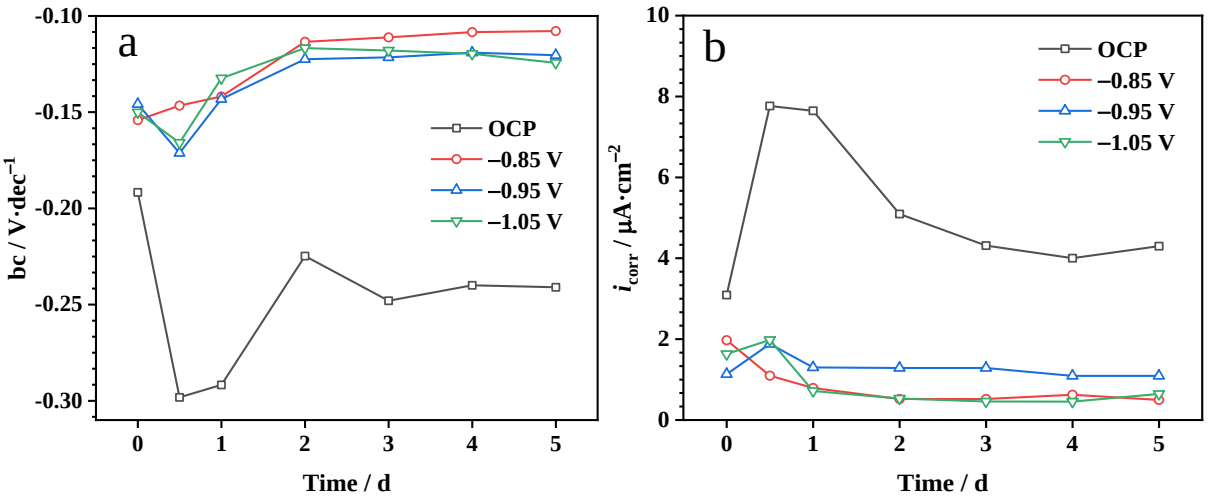

Figure 10. b_c (a) and i_{corr} (b) curves of AISI 4135 steel in strain GA-1-inoculated medium at OCP and after different pre-polarization potentials.

4. CONCLUSIONS

The effect of homoacetogenic bacteria, specifically strain *Blautia coccoides* GA-1, on AISI 4135 steel corrosion behaviour and cathodic protection was evaluated in this study. The following conclusions can be drawn from the obtained results:

(1) Strain GA-1 could consume cathodic hydrogen and promote the cathodic reaction of AISI 4135 steel, leading to the ennoblementof OCP.

(2) The corrosion rate was positively related to the number of strain cells. The hydrogen consumption of strain GA-1 was not the main reason behind the increase in corrosion current density.

(3) Pre-cathodic protection could effectively reduce the corrosion current density. The pre-cathodic protection's effects were similar at −0.85 V, −0.95 V and −1.05 V pre-polarization potentials in the presence of strain GA-1.

ACKNOWLEDGMENTS
This work was supported by the Joint Fund for Iron and Steel Research of National Natural Science Foundation of China and China Baowu Steel Group Corporation Ltd. (No. U1660112).

References

1. J.P. Hirth, *Metall. Trans. A*, 11 (1980) 861.
2. E. Akiyama, K. Matsukado, M. Wang, K. Tsuzaki, *Corros. Sci.*, 52 (2010) 2758.
3. P. Domżalicki, E. Lunarska, J. Birn, *Mater. Corros.*, 58 (2015) 413.
4. E. Ohaeri, U. Eduok, J. Szpunar, *Int. J. Hydrogen Energy*, 43 (2018) 14584.
5. T.M. Zhang, W.M. Zhao, T.T. Li, Y.J. Zhao, Q.S. Deng, Y. Wang, W.C. Jiang, *Corros. Sci.*, 131 (2018) 104.
6. P. Yin, X. Li, W. Lu, Y. Chen, Z. Yang, B. Zhang, Y. Guo, J. Ding, R. Cao, *Int. J. Electrochem. Sci*, 14 (2019).
7. E. Lunarska, J. Birn, P. Domżalicki, *Mater. Corros.*, 58 (2007) 13.
8. T. Wu, M. Yan, D. Zeng, J. Xu, C. Sun, C. Yu, W. Ke, *Corros. Sci.*, 91 (2015) 86.
9. D. Wang, F. Xie, M. Wu, D. Sun, X. Li, J. Ju, *Int. J. Hydrogen Energy*, 42 (2017) 27206.
10. Y. Zhu, Y. Huang, C. Zheng, Q. Yu, *Mater. Corros.*, 58 (2007) 447.
11. H.T. Dinh, J. Kuever, M. Mussmann, A.W. Hassel, M. Stratmann, F. Widdel, *Nature*, 427 (2004) 829.
12. L. Yu, J. Duan, X. Du, Y. Huang, B. Hou, *Electrochem. Commun.*, 26 (2013) 101.
13. H. Venzlaff, D. Enning, J. Srinivasan, K.J.J. Mayrhofer, A.W. Hassel, F. Widdel, M. Stratmann, *Corros. Sci.*, 66 (2013) 88.
14. M.T. Madigan, J.M. Martinko, K.S. Bender, D.H. Buckley, D.A. Stahl, T. Brock, Brock biology of microorganisms 14th edn, Pearson, (2015) Essex, England.
15. G. Diekert, G. Wohlfarth, *Antonie Van Leeuwenhoek*, 66 (1994) 209.
16. J. Li, L. You, C. Liu, Q. Ban, *Science and Technology Review (in Chinese)*, 31 (2013) 20.
17. C. Liu, J. Li, Y. Zhang, A. Philip, E. Shi, X. Chi, J. Meng, *J. Ind. Microbiol. Biotechnol.*, 42 (2015) 1217.
18. E. Marsili, J.B. Rollefson, D.B. Baron, R.M. Hozalski, D.R. Bond, *Appl. Environ. Microbiol.*, 74 (2008) 7329.
19. C.I. Torres, A.K. Marcus, H.-S. Lee, P. Parameswaran, R. Krajmalnik-Brown, B.E. Rittmann, *FEMS Microbiol. Rev.*, 34 (2010) 3.
20. R. Javaherdashti, Microbiologically Influenced Corrosion (MIC). In: Microbiologically Influenced Corrosion, Springer, Cham, (2017), pp. 29.
21. F.M. AlAbbas, C. Williamson, S.M. Bhola, J.R. Spear, D.L. Olson, B. Mishra, A.E. Kakpovbia, *Int. Biodeterior. Biodegrad.*, 78 (2013) 34.
22. J.S. Liao, H. Fukui, T. Urakami, H. Morisaki, *Corros. Sci.*, 52 (2010) 1393.
23. D. Starosvetsky, R. Armon, J. Yahalom, J. Starosvetsky, *Int. Biodeterior. Biodegrad.*, 47 (2001) 79.
24. J. Wang, X. Li, W. Wang, *Journal of Chinese Society for Corrosion and Protection*, 24 (2004) 262.
25. L. Kotovsky, R. Baillargeon, O. Baujard, V. Baujard, S. Aurel, C. Boyer, R.D. Appel, V. Feliu, J.A. Gonzalez, C. Andrade, *Corros. Sci.*, 40 (1998) 975.
26. F.M. Alabbas, C. Williamson, S.M. Bhola, J.R. Spear, D.L. Olson, B. Mishra, A.E. Kakpovbia, *Int. Biodeterior. Biodegrad.*, 78 (2013) 34.

27. L. Hao, S. Zhang, J. Dong, W. Ke, *Corros. Sci.*, 58 (2012) 175.
28. T. Wu, J. Xu, M. Yan, C. Sun, C. Yu, W. Ke, *Corros. Sci.*, 83 (2014) 38.
29. T. Wu, J. Xu, C. Sun, M. Yan, C. Yu, W. Ke, *Corros. Sci.*, 88 (2014) 291.
30. C. Cao, Principles of Electrochemistry of Corrosion 3th edn, Chemical Industry Press, (2008) Beijing, China.
31. J.W. Sowards, E. Mansfield, *Corros. Sci.*, 87 (2014) 460.
32. A. Heyer, F. D'Souza, X. Zhang, G. Ferrari, J.M.C. Mol, J.H.W. de Wit, *Biodegradation*, 25 (2014) 67.
33. E. Ohaeri, U. Eduok, J. Szpunar, *Int. J. Hydrogen Energy*, 43 (2018) 14584.
34. T.M. Zhang, W.M. Zhao, T.T. Li, Y.J. Zhao, Q.S. Deng, Y. Wang, W.C. Jiang, *Corros. Sci.*, 131 (2018) 104.
35. C. Batt, J. Dodson, M. Robinson, *Br. Corros. J.*, 37 (2002) 194.
36. B. Da Silva, F. Salvio, D. Dos Santos, *Int. J. Hydrogen Energy*, 40 (2015) 17091.